Cloud Publications
International Journal of Advanced Packaging Technology
2017, Volume 5, Issue 1, pp. 258-266
ISSN 2349-6665, doi 10.23953/cloud.ijapt.28

Case Study

Open Access

Low Cost Temperature & Humidity Chamber

Erica Thomas, Siripong Malasri, Robert Moats, and Dustin Schrecongost

Healthcare Packaging Consortium, Christian Brothers University, 650 East Parkway South, Memphis, TN, USA

Correspondence should be addressed to Siripong Malasri, pong@cbu.edu

Publication Date: 24 January 2017

DOI: https://doi.org/10.23953/cloud.ijapt.28

Abstract A low-cost 56 ft^3 temperature/humidity chamber was built from 2-inch thick extruded polystyrene (XPS) foam. Commercially available instruments were used, including space heater, humidifier, and temperature/humidity data logger. Due to the inaccurate control of home-use heater and humidifier, environmental condition in the chamber was different from the setting condition. Thus, thirty different combinations of temperature ranging from 70-90 $^\circ F$ and relative humidity ranging from 50-75% were used with actual conditions recorded by the data logger. A calibration spreadsheet was then developed using an artificial neural network to instruct the user to set environmental conditions for desired conditions. The neural network spreadsheet predicted temperature and relative humidity within 3% and 2% errors, respectively.
Keywords *Temperature/Humidity Chamber; Environmental Chamber; Artificial Neural Network*

1. Introduction

The CBU packaging test laboratory has had a commercial environmental chamber since 2005 with a controller upgrade in 2016. Since the laboratory has become an ISTA certified packaging test lab in 2009, the chamber has been regularly used for various commercial testing projects. There was a need for the second chamber for R&D projects that do not require the sophistication of an expensive commercial chamber. Thus, a low-cost environmental chamber as described in this article was built from commercially available materials and instruments for under 1,000USD. Table 1 shows a comparison of features between this low-cost chamber and the exiting commercial chamber.

Table 1: *Low-Cost Chamber versus Commercial Chamber*

Feature	Low-Cost Chamber	Commercial Chamber
Cost	Under 1,000USD	Over 30,000USD
Chamber Volume (Interior Dimensions)	56 ft^3 (44"X48"X46")	32 ft^3 (38"X38"X38")
Temperature Range	70 to 90 $^\circ F$	-49 to 374 $^\circ F$

Relative Humidity Range	50 to 75%	10 to 98%
Profile Setting	One setting	Multiple settings
Temperature Setting Increment	$1^{\circ}F$	$0.1^{\circ}F$
Relative Humidity Setting Increment	5%	0.1%
Footprint	48”X52”	48”X72”
Height	50”	92”
Portability	Yes	No

2. Materials and Methods

Figure 1 shows instruments used in building the low-cost chamber.

- Heater [1]: Automatic temperature control with 750/1500 watts (120USD)
- Humidifier [2]: Ultrasonic warm and cool mist humidifier with auto humidistat and timer (124USD)
- Temperature/Humidity Data Logger [3]: 16,000 humidity and 16,000 temperature readings with a user programmable sample rate and analysis software. Temperate range: -40 to 158 $^{\circ}F$. Relative humidity range: 0 to 100% (128USD)
- Small Fan: For air circulation inside the chamber (12USD)
- Tablet: For calibration spreadsheet (50USD)

Figure 1: *Commercially Available Instruments*

The body of the chamber was built from a 2-inch thick Owens Corning R-10, Foamular 250, energy-saving moisture-resistant extruded polystyrene (XPS) foam [4] as shown in Figure 2. Door was attached to the chamber body via industry-grade Velcro. A 7-inch Android tablet for calibration spreadsheet was mounted next to the chamber. Figure 2 also shows the layout of instruments, with the data logger attached to the right interior side wall.

Figure 2: *Chamber Details*

Two methods were used to ensure that no moisture was absorbed by the XPS foam. In the first method, several XPS specimens were placed in the commercial chamber (at 73 $^{\circ}F$ and 90% relative humidity (RH)), as shown in the left image of Figure 3. They were weighed daily with 0.0001 gram accuracy for five consecutive days and no weight change was observed. In the second method, a tube filled with water was secured above a piece of XPS. The bottom of the tube was sealed to prevent leakage, while the top was covered to prevent evaporation, as shown in the right image of Figure 3. The water level was observed daily for five consecutive days. No change was observed. Thus, the XPS moisture-resistance was validated.

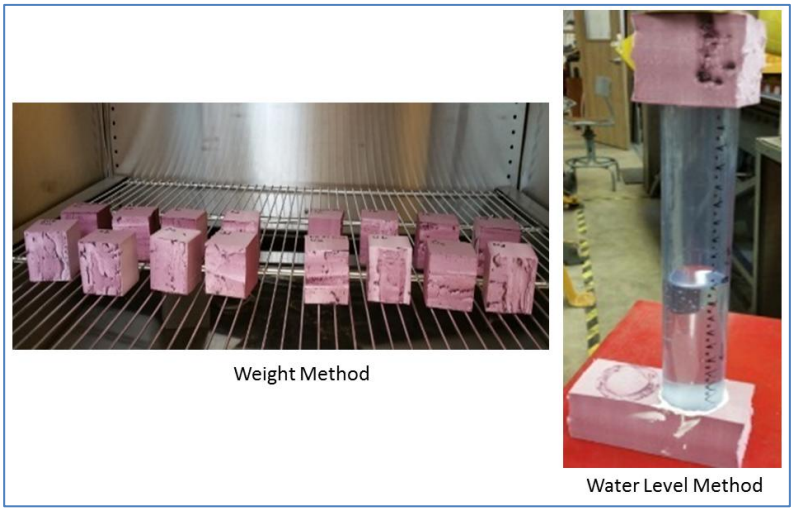

Figure 3: *XPS Moisture-Resistant Verification*

Chamber calibration consisted of collecting 16 to 18 hours of data every one minute for 30 different temperature-humidity combinations ranging from 70-90 $^{\circ}F$ and 50-75% RH, in 5 $^{\circ}F$ and 5% RH

increments, respectively. Tests were run for four days per week over the course of three months. Data was downloaded from the data logger after each test. Ten to 14 hours of the 16 to 18 hours of data collected were used to generate measurements of average chamber operating temperature and relative humidity values given specified heater/ humidifier settings. Only 10 to 14 hours of the data were used because four to six hours were needed for the chamber to reach a steady condition.

Data for each temperature-RH combination was downloaded and averaged, with the maximum, minimum, and range recorded for each testing day. After data for all 30 temperature-RH combinations were collected; scatter plots, trend lines, and trend line equations were produced to establish general chamber temperature and RH calibration charts (see Figure 4 and Figure 5).

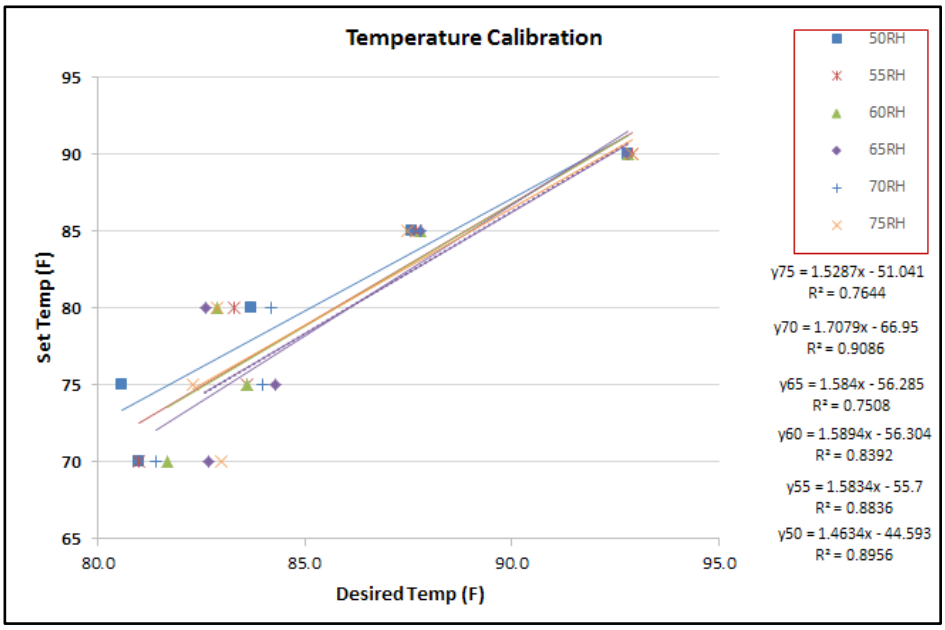

Figure 4: *Temperature Calibration Chart*

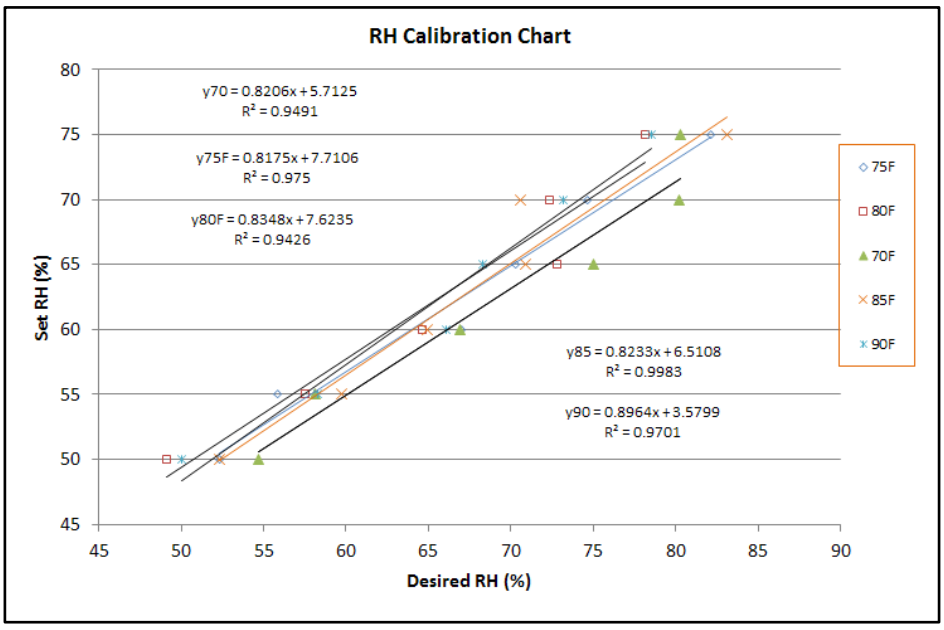

Figure 5: *RH Calibration Chart*

Training data set was then generated from these trend line equations for use with NeuroShell2 neural network software [5]. A feed-forward fully-connected backpropagation neural network shown in Figure 6 was used. The numbers of input and output neurons were controlled by the collected data, i.e., two input parameters (desired temperature and desired RH) and two output parameters (set temperature and set RH). The number of hidden neurons was arbitrary and was chosen as seven in this work.

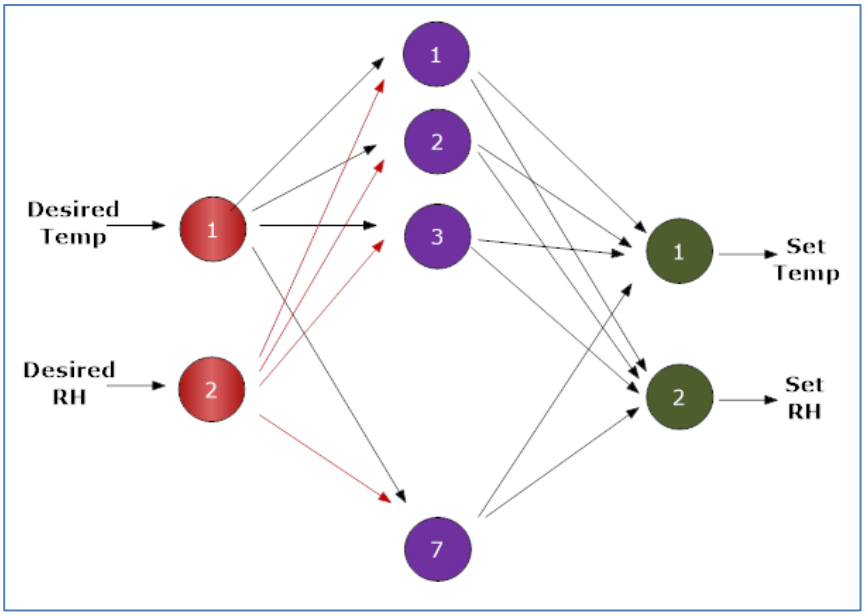

Figure 6: *Calibration Neural Network*

3. Results and Discussion

Table 2 summarizes training data, neural network predicted value, and % errors.

- Column 1 **Case**: Thirty cases were used in developing the neural network calibration software.
- Column 2 **Desired Temp**: This is the desired temperature in the chamber.
- Column 3 **Desired RH**: This is the desired RH in the chamber
- Column 4 **Set Temp**: This is the set temperature on the heater. It should be noted that this is not the raw data collected. It is the value generated from a trend line equation shown in Figure 4.
- Column 5 **Set RH**: This is the set RH on the humidifier. It should be noted that this is not the raw data collected. It is the value generated from a trend line equation shown in Figure 5.
- Column 6 **Mark**: The code 'T' indicates that the data is for training.
- Columns 7 & 8 **NN Set Temp** & **NN Set RH**: These are the set temperature and set RH predicted by the neural network.
- Column 9 & 10 Temp Error & **RH Error**: These are the errors for temperature and RH predictions.

The neural network predicts temperature with an error range of 0 – 2.70% and average error of 0.75%. It predicts relative humidity with an error range of 0.05 – 1.26% and average error of 0.49%.

Table 2: *Performance of Neural Network Calibration Software*

1	2	3	4	5	6	7	8	9	10
Case	**Desired Temp ($^{\circ}F$)**	**Desired RH (%)**	**Set Temp ($^{\circ}F$)**	**Set RH (%)**	**Mark**	**NN Set Temp ($^{\circ}F$)**	**NN Set RH (%)**	**Temp Error (%)**	**RH Error (%)**
1	70	50	58	47	'T'	57	48	2.51	1.26
2	70	55	55	51	'T'	56	51	1.66	0.47
3	70	60	55	55	'T'	55	55	0.52	0.16
4	70	65	55	59	'T'	55	59	0.66	0.72
5	70	70	53	63	'T'	54	63	2.70	0.54
6	70	75	56	67	'T'	55	68	1.88	0.75
7	75	50	65	49	'T'	65	49	0.62	0.67
8	75	55	63	53	'T'	64	53	1.33	0.68
9	75	60	63	57	'T'	63	57	0.10	0.55
10	75	65	63	61	'T'	62	61	1.26	0.05
11	75	70	61	65	'T'	62	65	1.88	0.17
12	75	75	64	69	'T'	63	69	0.94	0.05
13	80	50	72	49	'T'	72	49	0.51	0.32
14	80	55	71	54	'T'	71	54	0.70	0.85
15	80	60	71	58	'T'	71	58	0.51	0.70
16	80	65	70	62	'T'	70	62	0.35	0.13
17	80	70	70	66	'T'	70	66	0.16	0.28
18	80	75	71	70	'T'	72	70	0.78	0.51
19	85	50	80	48	'T'	80	48	0.13	0.39
20	85	55	79	52	'T'	79	52	0.53	0.08
21	85	60	79	56	'T'	79	56	0.44	0.63
22	85	65	78	60	'T'	78	60	0.23	0.19
23	85	70	78	64	'T'	78	64	0.11	0.20
24	85	75	79	68	'T'	79	68	0.39	0.49
25	90	50	87	48	'T'	87	48	0.01	0.27
26	90	55	87	53	'T'	87	52	0.11	1.16
27	90	60	87	57	'T'	87	58	0.30	0.97
28	90	65	86	62	'T'	86	62	0.56	0.21
29	90	70	87	66	'T'	87	66	0.46	0.54
30	90	75	87	71	'T'	87	70	0.00	0.83
							Min =	*0.00*	*0.05*
							Max =	*2.70*	*1.26*
							Avg =	*0.75*	*0.49*

The algorithm of the calibration software was generated from NeuroShell2 software (Appendix A) and programmed into an Excel spreadsheet as shown in Figure 7. In order to test the generalizability of the neural network algorithm the spreadsheet was used to generate data for an RH of 52.5%, which was not used in training. Figure 8 shows a temperature calibration chart with RH of 52.5%, generated by the calibration spreadsheet, plotting between an RH of 50% and 55%. Similarly, the generalizability was shown on RH calibration chart using a temperature of 72.5 $^{\circ}F$ (Figure 9).

	A	B	C	D
7	netsum			
8	feature2(7)			
9				
10	Note - the following are names of inputs and outputs:			
11	Note - inp(1) is AT	Desired Temperature (F)	80	Input
12	Note - inp(2) is ARH	Desired RH (%)	55	Input
13	Note - outp(1) is ST	Set Temperature (F)	71	Output
14	Note - outp(2) is SRH	Set RH (%)	54	Output
15				
16	if (inp(1)<70) then inp(1) = 70			
17	if (inp(1)>90) then inp(1) = 90			
18	inp(1) = (inp(1) - 70) /20	inp(1)	0.5	
19				
20	if (inp(2)<50) then inp(2) = 50			

Figure 7: *Calibration Excel Spreadsheet*

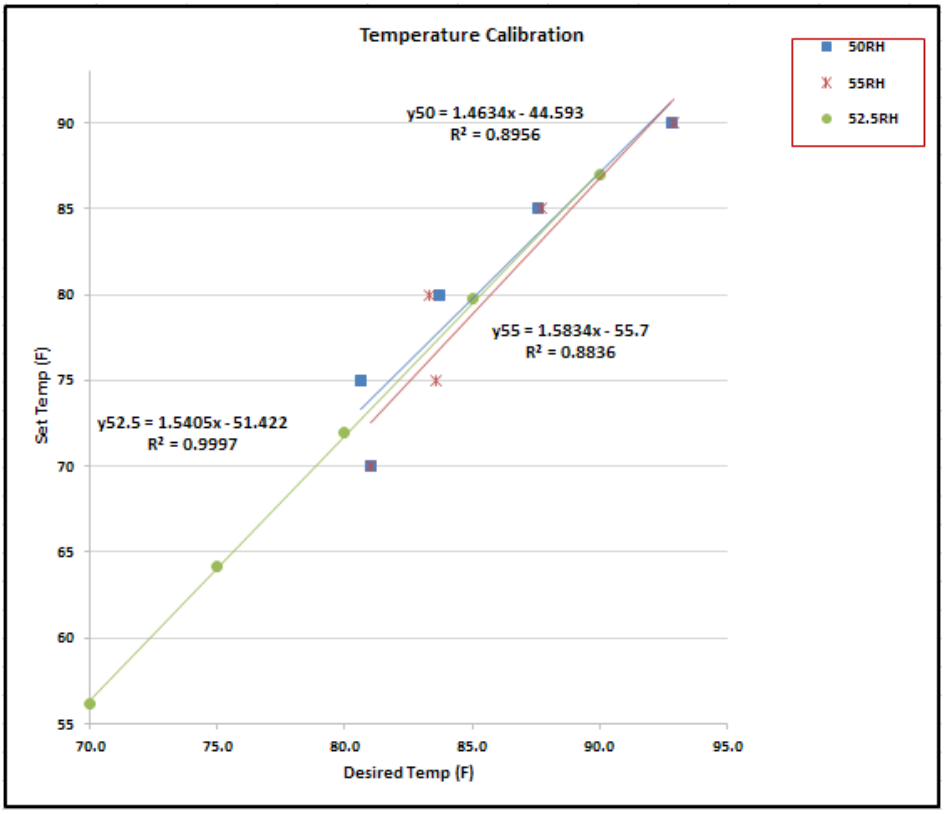

Figure 8: *Generalization of the Calibration Software Shown on Temperature Calibration Chart*

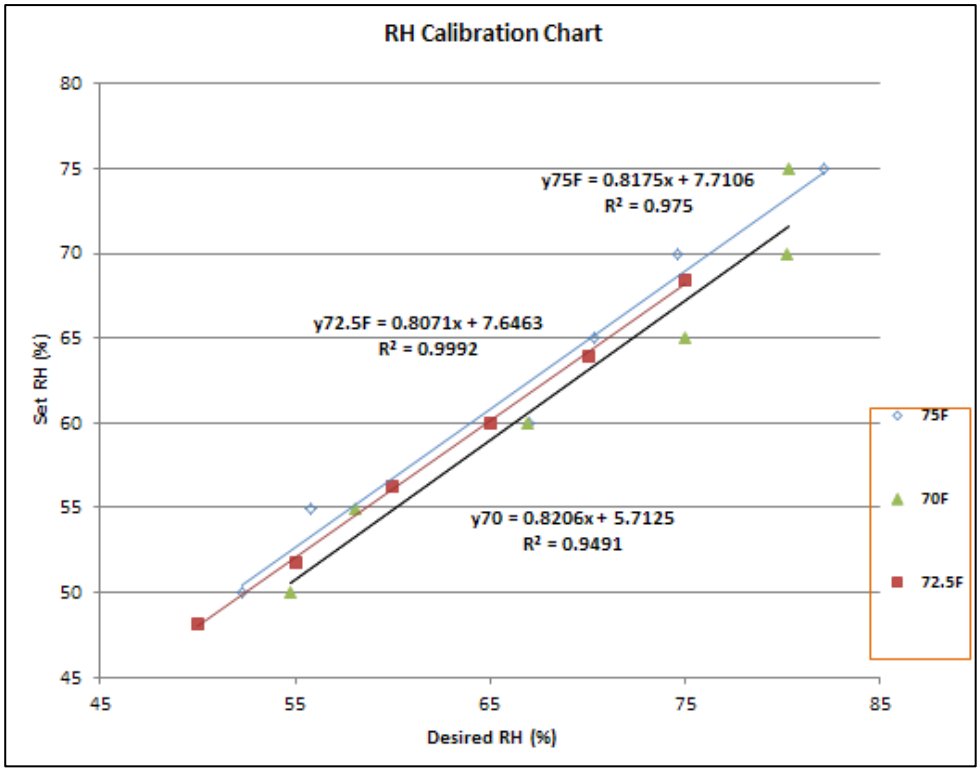

Figure 9: *Generalization of the Calibration Software Shown on Relative Humidity Calibration Chart*

4. Conclusion

This study demonstrates that the construction of a reliable and inexpensive temperature/humidity chamber using readily available materials is possible. Commercial chambers, depending on size, can have a starting price tag of 30,000USD. The chamber constructed for this study cost less than 1,000USD and can simulate temperature and relative humidity conditions that fall within the temperature-RH ranges tested with a percent error of less than 5%. Further testing of additional temperature-RH combinations would increase the reliability of setting temperatures and RH values for the heater and humidifier used in this study. However, it should be noted that temperature and humidity results do not necessarily transfer, even if a second chamber were to be built in exactly the same way, using the same components. All chambers require calibration.

Additionally, because residential grade heater and humidifier devices were used, temperature and humidity levels are constrained by the range and setting mode of the device. In this study, the heating range tested was from 70-90$^{\circ}F$ using only 5$^{\circ}F$ increments. The heater could have run using 1$^{\circ}F$ increments, and as a result, can provide additional parameters for testing. The humidifier chosen for this study was tested using a relative humidity range of 50-75% RH. Unlike the heater, the operational increments for the humidifier were limited to 5% increments. Consequently, if an experiment were to require a relative humidity setting between the 5% increments, the value would require rounding, which could influence the outcome of chamber interior condition.

Given the functional limitations of residential grade heating and humidifying devices, it is important to consider the level of accuracy required. However, use of the artificial neural network proved invaluable in its ability to interpolate - providing setting temperature and RH values, for temperature and humidity parameters not previously tested. Thus, while the choice of heater or humidifier may limit setting values, the use of an artificial neural network can advance the range of settings. Finally,

if the percentage of error presented in this study is within reason, constructing and calibrating a low-cost temperature/ humidity chamber might be a reliable alternative.

References

[1] *Vornado Heater Owner's Guide*. https://images-na.ssl-images-amazon.com/images/I/818PuYfw0PS.pdf. *Access date: December 28, 2016.*

[2] *PureGuardian Ultrasonic Humidifier Use & Care Instructions*. https://www.guardiantechnologies.com/uploads/H8000_manual.pdf. *Access date: December 28, 2016.*

[3] *EXTECH Humidity/Temperature Datalogger Product Datasheet*. http://www.extech.com/resources/RHT20_DS-en.pdf. *Access date: December 28, 2016.*

[4] *Owens Corning Foamular Energy-Saving, Moisture-Resistant XPS Insulation*. http://www.owenscorning.com/NetworkShare/EIS/10010242-FOAMULAR-XPS-101-Commercial-Brochure.pdf. *Access date: December 28, 2016.*

[5] *Ward Systems Group, Inc. NeuroShell2*. http:www.wardsystems.com/neuroshell2.asp. *Access date: December 25, 2015.*

Appendix A Generic Source Code Generated by NeuroShell2

```
netsum
 feature2(7)
Note - the following are names of inputs and outputs:
Note - inp(1) is AT
Note - inp(2) is ARH
Note - outp(1) is ST
Note - outp(2) is SRH
if (inp(1)<70) then inp(1) = 70
if (inp(1)>90) then inp(1) = 90
inp(1) = (inp(1) - 70) /20
if (inp(2)<50) then inp(2) = 50
if (inp(2)>75) then inp(2) = 75
inp(2) = (inp(2) - 50) /25
netsum = -3.070898
netsum = netsum + inp(1) * 4.10027
netsum = netsum + inp(2) * -1.408727
feature2(1) = 1 / (1 + exp(-netsum))
netsum = 0.2558365
netsum = netsum + inp(1) * -0.4038733
netsum = netsum + inp(2) * -3.089265
feature2(2) = 1 / (1 + exp(-netsum))
netsum = -0.6637989
netsum = netsum + inp(1) * -3.811205
netsum = netsum + inp(2) * 0.6173124
feature2(3) = 1 / (1 + exp(-netsum))
netsum = -22.38877
netsum = netsum + inp(1) * 9.987292E-02
netsum = netsum + inp(2) * 26.78505
feature2(4) = 1 / (1 + exp(-netsum))
netsum = 12.07675
netsum = netsum + inp(1) * -14.85412
netsum = netsum + inp(2) * -0.6312295
feature2(5) = 1 / (1 + exp(-netsum))
netsum = -14.60969
netsum = netsum + inp(1) * 13.47738
netsum = netsum + inp(2) * 0.8668328
feature2(6) = 1 / (1 + exp(-netsum))
netsum = -2.918397
netsum = netsum + inp(1) * -4.432046
netsum = netsum + inp(2) * 0.7326113
feature2(7) = 1 / (1 + exp(-netsum))
netsum = 0.7137885
netsum = netsum + feature2(1) * 1.945597
netsum = netsum + feature2(2) * -0.3679988
netsum = netsum + feature2(3) * -4.390033
netsum = netsum + feature2(4) * 0.3530397
netsum = netsum + feature2(5) * -0.4985445
netsum = netsum + feature2(6) * 1.220905
netsum = netsum + feature2(7) * -1.870898
outp(1) = 1 / (1 + exp(-netsum))
netsum = 0.3879333
netsum = netsum + feature2(1) * -0.7902336
netsum = netsum + feature2(2) * -5.173065
netsum = netsum + feature2(3) * -1.050403
netsum = netsum + feature2(4) * 0.8617824
netsum = netsum + feature2(5) * 0.9966981
netsum = netsum + feature2(6) * 2.90973
netsum = netsum + feature2(7) * -1.400668
outp(2) = 1 / (1 + exp(-netsum))
outp(1) = 34 *  (outp(1) - .1) / .8  + 53
outp(2) = 24 *  (outp(2) - .1) / .8  + 47
```

Cloud Publications
International Journal of Advanced Packaging Technology
2017, Volume 5, Issue 1, pp. 267-274
ISSN 2349-6665, Crossref: 10.23953/cloud.ijapt.318

Research Article

Evaluation of Containment Force Variability between Different Grades of Stretch Film

Kyle D. Dunno, Jake Wyns, John Cook

Atlantic Packaging Corporation 12201 Steele Creek Road Charlotte, NC 28273, USA

Publication Date: 25 October 2017

DOI: https://doi.org/10.23953/cloud.ijapt.318

Abstract Containment force is a measurement often used to qualify stretch films when they are applied to a unit load of packaged product. This measurement records the amount of resistance force a stretch film delivers when being displaced a specified distance. It has been the industry perception there are quality differences between commodity and high-performance grade stretch films. These perceived quality differences are believed to affect the variability between different grades when being examined in a laboratory. In order to evaluate this theory, two different grades of stretch film from two different manufacturers were applied to an instrumented test pallet and the containment force was measured. Results from this study showed there were no statistical differences between the variability of containment forces of different grades of stretch film between the same manufacturers. While the study was limited to only two manufacturers, the results indicated there is less variability between commodity and high-performance grade stretch films than was originally theorized. Additionally, it was observed that a predetermined containment force measurement of 25 lbs. could be obtained through a variety of different stretch wrapping parameters and equipment settings. Many of the developed patterns and settings used would have resulted in load shifting and/or load failures during actual transport. As a result of these observations, it was recommended to use containment force measurements as part of a quality assurance program and not a predictor of success during transportation.
Keywords *Containment force; Stretch film; Unit load*

1. Introduction

Packaged products are transported throughout the supply chain using a variety of complex distribution channels in order to deliver the goods to the consumer (Dunno, 2014). The primary method for distributing goods through the supply chain is to arrange and unitize packaged products onto a pallet for shipment. The most common material used in the transport packaging industry to unitize loads is stretch wrap (Rogers, 2011). Stretch wrap is a ductile plastic film that is wrapped around a unitized load of packaged products. Stretch film can be applied to a unit load either manually or through an automated process. Today, stretch films are engineered and designed to increase load containment and stability of the cargo (Pischel, 2017). Properly stretch wrapped loads begin by defining these parameters: load type, wrapping configuration and distribution environment (Singh et al., 2014). Figure 1 illustrates the different Load Profiles used to describe unitized loads.

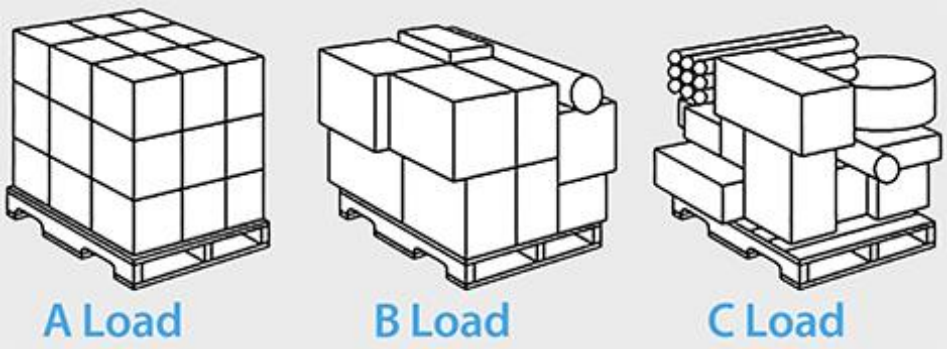

Figure 1: *Load profiles* (Stretch Film, 2017)

In very general terms, there are two types of stretch film produced and used within the packaging industry to secure loads for transport (Twede and Harte, 2011). These two categories are hand and machine films, which can be produced through a blown or cast extrusion process (Robertson, 2016). Regarding machine films, there are two common grades of stretch film produced, commodity grade and high-performance films. These films have different mechanical properties and can be engineered and designed for specific applications (Packaging Film Lab, 2017). It is presumed the two films would have different operating ranges and variability in performance when comparing commodity and high-performance grade films, but the data and science backing this theory is not readily available for users of stretch film.

Figure 2: *Highlight transportable test pallet*

One way to evaluate stretch film application is through measuring its containment force. Containment force is a common method used to measure the holding force of stretch film after it has been applied to a load of packaged products. This information can be easily obtained by following the protocol described in ASTM D4649 - Standard Guide for Selection and Use of Stretch Wrap Films (ASTM D4649-03, 2016). In this standard, a force plate and gauge are used to measure the containment force of the unit load. These systems can range from a simple steel plate or finger style tool with a force gauge to a complex system capable of measuring various film properties. One such complex system that can be used for evaluating stretch film application is the Highlight Transportable Test Pallet (Highlight Industries, Wyoming, and MI). Figure 2 illustrates the transportation test pallet system. This system is capable of collecting and measuring different stretch

film properties, including puncture, containment force, and compressive force, which are beneficial to both the manufacturer and end user of stretch films (Portable Electronic Equipment, 2017). In addition to determining film properties, this style of equipment can also be used as a quality control measurement device. As the equipment is designed to evaluate stretch film material properties, it is critical to understand the variability in the equipment used to evaluate these parameters.

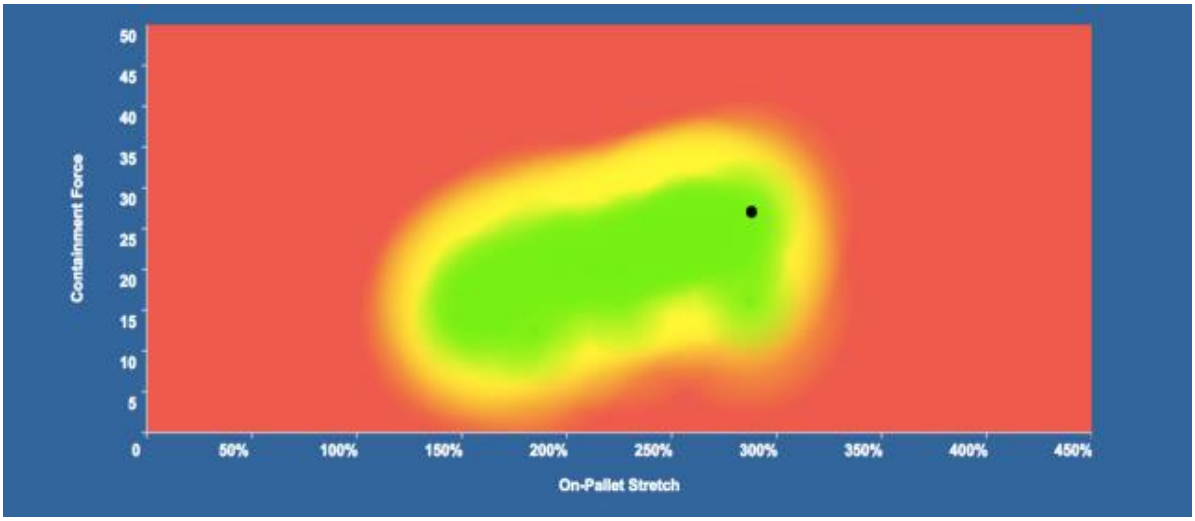

Figure 3: *Generalized heat map for high-performance stretch film*

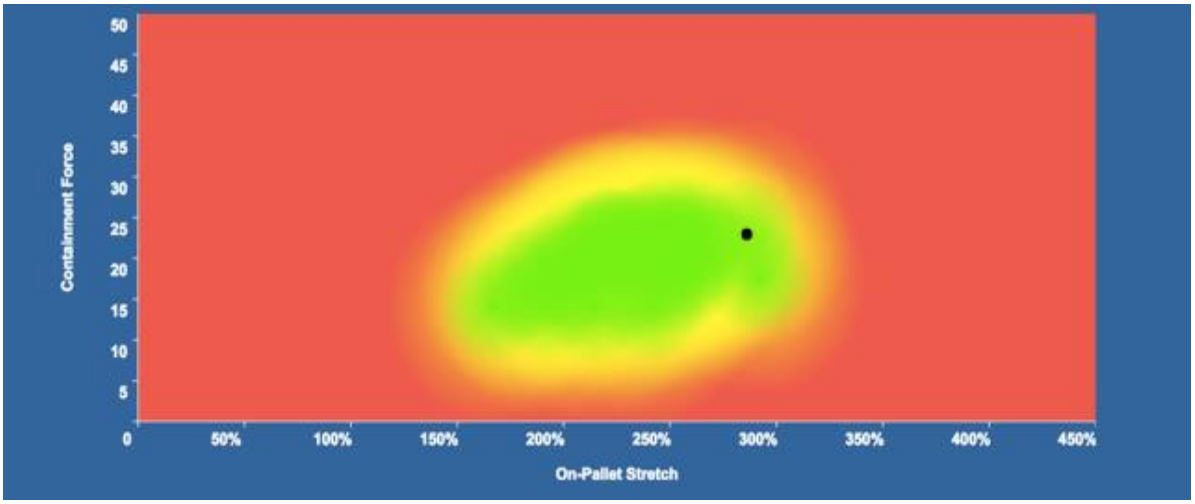

Figure 4: *Generalized heat map for commodity grade stretch film*

Containment force measurements can be useful during auditing and quality control, but lack correlation to field performance or application. The containment force is a quantifiable test method, but obtaining a specified containment force only indicates the system is in control. It doesn't indicate or predict the success of a wrapping pattern or film selection. As a result, the correlation between containment force and performance in the field needs to be investigated further as this is a critical knowledge gap that exists in the stretch film market.

The objectives of this research study were to evaluate the variation of the observed recordings and to determine the different wrap pattern combinations that can produce a similar containment force reading.

2. Materials and Methods

This evaluation involved two high-performance (HP) stretch films and two commodity grade (CG) stretch films, produced by a cast extrusion process. The HP films evaluated in this study were thinner in gauge than the corresponding CG stretch films. HP films for this study were categorized as having the ability to stretch beyond 275% ultimately having a wider working region of the film. Commodity films were described as having a lower operating and performance window. Figures 3 and 4 are developed heat maps which illustrate the general working regions for the two different grades of stretch film. The stretch films designated for this project are described in Table 1.

Table 1: *Stretch film properties*

Manufacturer	Material ID	Thickness (gauge)	Basis Wt. (GSM)	Roll Width (in.)
A	HP 1	51	50.3	20
B	HP 2	55	55.5	20
A	CG 1	70	72.4	20
B	CG 2	70	72.3	20

The selected films were applied to the perimeter of the Highlight Transportable Test Pallet using a Synergy 4 Highlight Stretch Wrapper (Highlight Industries, Wyoming, MI). Table 2 displays the stretch wrapper setup parameters used for this evaluation. Upon successful wrapping of the test pallet, the system was activated to perform the ASTM D4649 containment force test (ASTM D4649-03, 2016). The test is performed by extending a 6” diameter piston outward 4” at a constant rate. Upon full extension of the piston, the maximum containment force was obtained and recorded by the data acquisition system. This test sequence was performed ten times per film variable.

Table 2: *Stretch wrapper configuration*

Stretch Wrapper Parameters	
Number of top wraps	3
Pre-stretch (%)	250
On-pallet stretch	Positive
Turn table speed (rpm)	20
Carriage speed (%)	60
Number of revolutions	14

The stretch film identified as HP 1, was used to compare the different wrapping patterns and configurations to create a pre-determined containment value of 25 lbs. For this portion of the research project, the same roll of stretch film was used throughout the experiment. Here, as previously described earlier, the HP 1 stretch film was applied to the perimeter of the Highlight Transportable Test Pallet using a Synergy 4 Highlight Stretch Wrapper. Upon the completion of wrapping, the maximum containment force was obtained by the data acquisition software.

3. Results and Discussion

Results indicated the Highlight Data Acquisition Test Stand produced repeatable results which could be used to ensure quality control parameters of stretch film. To compare the variability between the two different grades of stretch film materials, a F-test for the Equality of Two Population Variances was computed with the data sets collected. Results from this analysis showed no statistical differences were observed between the variability of containment force for the two different grades of stretch films. Given the nature of the terminology used to describe these films, it was perceived commodity grade stretch films would have higher variability in the stretch parameters as compared to a higher performance stretch film. Observations from this study showed there was no statistical

difference in the variance between the two grades of materials, regardless of the terminology used to describe the film. Table 3 and Figures 5 and 6 show the results obtained from this analysis.

Table 3: *Load containment measurements*

ASTM Max Load Containment (lbs.)				
	Manufacturer A		Manufacturer B	
Test No.	HP	CG	HP	CG
1	21.0	23.5	20.7	20.1
2	21.5	23.4	21.5	20.9
3	21.8	23.2	20.7	20.5
4	21.6	23.4	23.1	20.5
5	23.1	22.9	20.8	20.6
6	22.0	24.4	21.6	20.4
7	21.7	23.7	22.7	20.2
8	22.6	23.2	20.7	19.7
9	21.8	23.0	20.8	19.9
10	21.5	23.0	20.7	19.9
Average	21.9	23.4	21.3	20.3
Std. Dev.	0.6	0.4	0.9	0.4

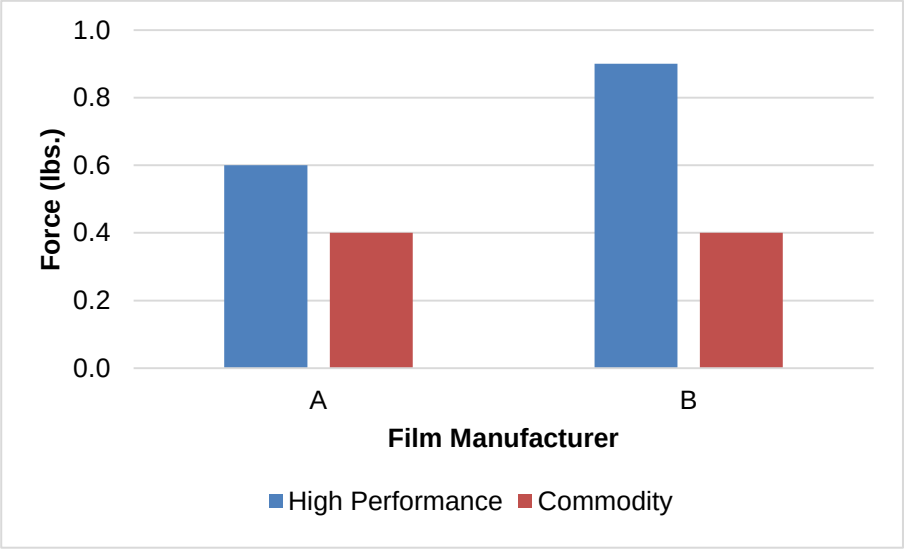

Figure 5: *Standard deviation in load containment measurements*

In addition to the containment force, the transportable test pallet as part of this study also measured the compressive forces of the stretch films. The high-performance films were of thinner gauge as compared to the commodity films evaluated in this study. The thinner gauge high-performance materials are being engineered to provide the better performance while additionally providing a more sustainable approach to unitizing loads. The measurements recorded illustrated the thinner gauge high-performance films could provide similar type compressive forces as those of thicker gauge materials (Figure 6). This was a key observation during this study as the transport industry continues to increase its usage of thinner gauge high-performance stretch films (Pischel, 2017). As such, it will be imperative for users of stretch film to understand how high-performance films correlate with commodity grade films.

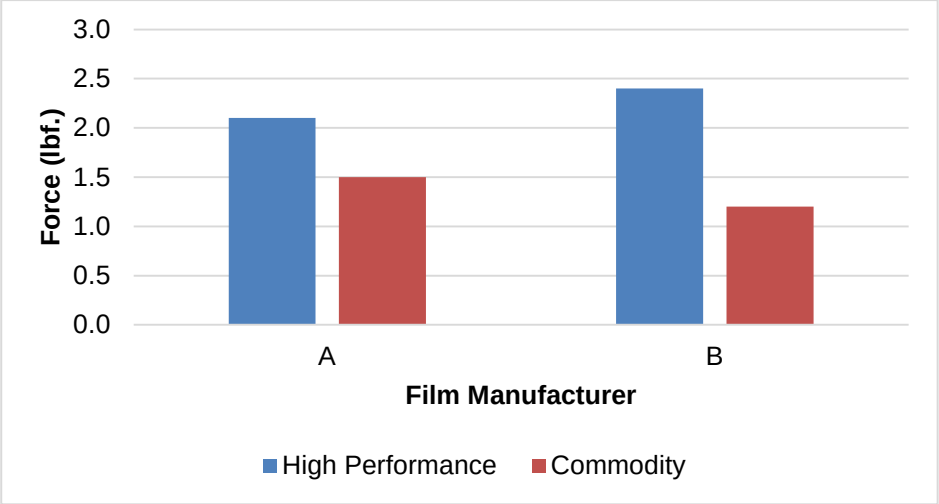

Figure 6: *Compressive force of stretch films*

Table 4: *Wrapping configurations executed using HP1 Stretch Film*

Pre-Stretch (%)	Pallet Stretch (%)	Top Wraps	Cut & Weigh (oz.)	Revolutions	Tension Force	ASTM Force (lbs.)
150	242	3	3.8	14	6.40	25.3
150	202	4	4.7	15	5.90	24.3
150	167	5	5.6	16	5.40	24.8
150	158	6	6.3	17	5.20	25.3
175	237	3	3.9	14	6.00	25.4
200	273	2	3.5	13	6.05	25.3
200	233	3	4.0	14	5.60	24.8
200	216	4	4.7	14	5.35	25.3
200	205	5	5.2	14	5.20	25.6
225	253	3	3.7	14	5.40	25.6
250	313	2	3.0	13	5.90	24.6
250	270	3	3.6	14	5.35	26.8
250	254	4	4.0	15	5.20	24.1
275	284	3	3.4	14	5.20	25.8
300	315	2	2.9	13	5.35	24.7
300	307	3	3.2	14	5.10	24.5
300	297	4	3.5	15	5.00	24.4

The containment force is a quantitative measurement of the system but is not always an indicator of application performance when looking at the performance of the load in the field. The containment force values are based on the number of film revolutions applied to the load and the tension at which the films are applied to the load. As a result of this, there were numerous patterns and wrapping configurations developed to generate the same containment force, but all may have different results during transport. Table 4 displays the number of wrapping configurations capable of producing a containment force of 25 lbs. In total, 17 different wrapping configurations were utilized in order to produce a maximum containment force value of approximately 25 lbs. Although certain wrapping

configurations displayed may be egregious, if obtaining a specified containment force is part of a quality assurance, these loads would be acceptable based on reaching a specified predetermined containment force value.

4. Conclusion

Conducted was an examination of the variability between two different grades of stretch films. An instrumented transportable test pallet was employed to measure containment force of the stretch films after application. Results showed the transportable test pallet was capable of reproducing repeatable results that could be used for quality assurance and control by stretch film manufacturers and end users.

Comparing the two different grades of film, no statistical difference existed between the variability of containment force across the samples evaluated. These results, which are only based on the data collected from this study, indicate there was not higher variability in containment force for the common grade stretch films, which was the perceived notion. Further research could be completed to compare variability of commodity and high-performance grade stretch films to incorporate multiple production runs and production locations.

The compressive forces measured during this analysis showed the high-performance stretch films compared favorably with the commodity stretch films. With the high-performance stretch films being thinner in gauge, the results from this data set indicate it is possible to obtain the same types of compressive forces as those offered by thicker gauge commodity films. Additionally, the thinner films are a more sustainable approach to unit load stability by reducing the total stretch film volume usage.

In addition to evaluating the variability of containment force, a number of different wrap configurations and patterns were developed in order to produce a particular containment force value of 25 lbs. The containment force value is a quantitative measurement, but does not necessarily correlate to performance during transport. To produce a maximum containment force value of 25 lbs., seventeen different wrapping patterns and/or configurations were employed. At this stage, the wrapping patterns were not compared to field performance, only showing the reader there are numerous configurations to produce a specified containment force value. This is valuable as it shows if only using containment force as a metric for performance, the stretch film user could potentially be unaware of changes in wrapping patterns which could potentially lead to a decrease in load stability.

References

ASTM D4649-03. 2016. *Standard Guide for Selection and Use of Stretch Wrap Films*. ASTM International, West Conshohocken, PA. Available from: *https://www.astm.org/Standards/D4649.htm*

Dunno, K. 2014. Effects of transportation hazards on package performance and food product shelf life. Available from: *http://tigerprints.clemson.edu/all_dissertations/1432*

Pischel, K. 2017. *Elimination of Shipping Damage through Stretch Film Optimization*. International Safe Transit Association TransPack Forum, Orlando, FL.

Packaging Film Lab - Atlantic Packaging. 2017.
Available from: *http://www.atlanticpkg.com/consulting/film_lab*

Portable Electronic Equipment - Highlight Industries Inc. 2017.
Available from: *http://www.highlightindustries.com/portable-electronic-equip*

Rogers, L.K. 2011. Keeping it together. *Modern Materials Handling*, pp.32-35.

Robertson, G.L. 2006. *Food Packaging: Principle and Practice*. Boca Raton, FL.: CRC Press.

Singh, J., Cernokus, E., Saha, K. and Roy, S. 2014. The effect of stretch wrap prestretch on unitized load containment. *Packag. Technol. Sci.*, 27, pp.944-961.

Stretch Film-Kyana Packaging Solutions. 2017
Available from: *http://www.arbaughmarketing.com/SCStretchFilm2.html*

Twede, D. and Harte, B. 2011. *Logistical Packaging for Food Marketing Systems*, in food and beverage packaging technology. 2nd ed. Coles, R. and Kirwan, M. (eds.), Oxford, UK: Wiley-Blackwell, pp.85-105.